Chemical and Structural Characterization of the Mineral Phase from Cortical and Trabecular Bone

A. Bigi, G. Cojazzi, S. Panzavolta, A. Ripamonti, N. Roveri, M. Romanello, K. Noris Suarez, and L. Moro

AB, SP, AR, NR. Dipartimento di Chimica "G. Ciamician," Università di Bologna, Bologna, Italy.—GC. Centro di Studio per la Fisica delle Macromolecole del C.N.R., c / o Dipartimento di Chimica "G. Ciamician," Università di Bologna, Bologna, Italy.—MR, KNS, LM. Dipartimento di Biochimica, Biofisica e Chimica delle Macromolecole, Università di Trieste, Trieste, Italy

Abstract

X-ray diffraction, infrared spectroscopy and chemical investigations have been carried out on the inorganic phases from rat cortical and trabecular bone. Although both inorganic phases consist of poorly crystalline B carbonated apatite, several significant differences have been observed. In particular, trabecular bone apatite displays reduced crystallite sizes, Ca / P molar ratio, and carbonate content, and exhibits a greater extent of thermal conversion into β-tricalcium phosphate than cortical bone apatite. These differences can be related to the different extents of collagen posttranslational modifications exhibited by the two types of bone, in agreement with their different biological functions. Journal of Inorganic Biochemistry 68, 45–51 (1997) © 1997 Elsevier Science Inc.

Introduction

The mineral phase of bone is constituted of poorly crystalline hydroxylapatite (HA), characterized by the presence of numerous foreign ions [1–3]. Among the bivalent ions which can be associated to biological apatites, magnesium displays noticeable importance, due to its relatively high presence and key structural role on hydroxylapatite [4–6]. Magnesium is known to inhibit apatite crystallization in solution [7], it can substitute for calcium into HA structure just up to about 10 atom % [6] and it is mainly adsorbed to the crystal surface. Whatever its location in the crystals, magnesium destabilizes the structure of HA and favors its thermal conversion into β-tricalcium phosphate (β-TCP) [5, 8, 9]. In calcified tissues, the amount of magnesium associated to the apatitic phase is higher at the beginning of the calcification process and decreases on increasing calcification [8–10].

Moreover, biological apatites usually contain appreciable amounts of carbonate. HA structure can host carbonate ions at two different sites: site A, where they substitute for OH^- ions, and site B, where they replace PO_4^{3-} groups [11–13] The presence of carbonate, which in biological apatites usually occupy B sites, can reduce the destabilizing effect of some ions, such as magnesium, on HA structure [14, 15].

Biological apatites from different normal and pathological calcified tissues, at different degrees of calcification, exhibit different chemical composition, crystallinity and stability [2, 16]. Among the factors affecting the mineralization process, crystal size displays an important role because it determines the surface area and, as a consequence, influences the stoichiometry and the solubility properties of biological apatites [17]. In normal calcified tendons and bone, magnesium and acid phosphate contents decrease, whereas carbonate content, Ca/P molar ratio, crystallite sizes and stability of HA increase with increasing calcification [9, 10, 18, 19]. Furthermore, biochemical analysis of the maturing bone reveals a progressive increase in the amount of mineral and a relative decrease in bone matrix, although the amount of collagen in the matrix increases [10].

Since collagen fibrils represent the structural macromolecules of calcified collagenous tissues, the observed differences in the mineral component could be related to collagen modifications. In the perinatal lethal form of osteogenesis imperfecta the decrease in collagen content, which leads to an abnormal collagen framework, is associated with an abnormal mineralization of bone [20]. Furthermore, the Ca/P molar ratio and the sizes of the apatitic crystallites associated with collagen in osteogenesis imperfecta have been found to be smaller than in normal collagen [21, 22]. Finally, a direct relationship between pyridinium cross-links concentration and bone mineral density has been verified in osteoporotic bone [23].

Recently, Noris Suarez et al. [24] reported different extents of collagen posttranslational modifications in rat cortical and trabecular bone. Cortical bone contains a higher amount of hydroxylysine residues and pyridinium cross-links concentration, while trabecular bone displays a higher glycosylation of hydroxylysine. The lower number of pyridinium cross-links in trabecular bone collagen suggests that fibrils have a reduced stability, whereas cortical bone matrix would appear to be more stable due to the larger number of nonreducible cross-links conferring mechanical strength to the bone structure. These findings are not surprising in view of the different func-

tions fulfilled by cortical and trabecular bone. Any alter-ation in the size and tensile strength of the collagen fibrils could affect the nucleation site for mineral forma-tion [25], or, however, the site where mineral deposition occurs. On this basis it is hypothesized that the mineral in these two collagenous matrices would differ.

In order to verify this hypothesis, we have carried out a chemical and structural characterization of the mineral phases isolated from rat cortical and trabecular bone. The results put into evidence several differences which can be interpreted as due to different degrees of maturation of trabecular and cortical bone.

Materials and Methods
Animals

Ten female 100-day-old Sprague-Dawley rats were sacri-ficed under anesthesia and tibias and femurs were re-moved and dissected free of adhering tissue.

Tissue Preparation

Bones were dissected into two anatomically distinct areas: the diaphysis containing only cortical bone and the meta-physis from which trabecular bone was scraped. The periosteum was stripped from the diaphysis and the corti-cal bone was fragmented.

Air dried samples were ground in an agate mortar only for a few minutes to avoid sample heating. The powders were successively seived to a mean diameter comprised between 0.18 and 0.32 mm.

The analysis of the inorganic phase was carried out on cortical and trabecular samples deproteinated with warm hydrazine hydroxide [9], which, according to J. D. Ter-mine et al. [26], induces no alteration in the structural properties of the mineral phase. Part of the powdered samples was heat-treated at 1000°C for 15 h.

Methods

Powder X-ray diffraction analysis of deproteinated sam-ples was carried out by means of a Philips PW 1050/81 powder diffractometer equipped with a graphite monochromator in the diffracted beam. CuKα radiation was used. The 2ϑ range was from 10 to 65° at a scanning speed of 0.5°/min. The lattice constants were determined by least square refinements.

In order to evaluate the crystal size of the apatitic crystallites, further x-ray diffraction data were obtained in two regions, peak (002) between 24.4 and 27.4° of 2ϑ and peak (310) between 37.4 and 41.5° of 2ϑ, by means of step scans using a fixed counting time period of 30 seconds and a scan rate of 0.1°/step.

For i.r. absorption analysis, 1 mg of the powdered samples was carefully mixed with 300 mg of KBr (in-frared grade) and pelleted under vacuum. The pellets were analyzed using a Perkin Elmer 380 ir Grating Spectrophotometer, range 4000–400 cm, normal slit and scanning speed of 72 cm^{-1}/min.

Thermogravimetric analysis was carried out on pow-dered samples using a Perkin Elmer TG-7 equipped with a P.E. 3700 Data Station. Heating was performed in a platinum crucible in air flow (20 cm^3/min) at a rate of 5°/min up to 900°C. The samples weights were in the range 5–10 mg.

Calcium and magnesium content were determined us-ing an atomic absorption spectrophotometer (Perkin Elmer 373); ashed tissues were diluted to an appropriate volume with 10% lanthanum in 50% HCl.

Phosphorus content was determined spectrophotomet-rically as molybdovanadophosphoric acid [27].

Results

The inorganic phase content of the samples was deter-mined from the results of thermogravimetric analysis. The TG-DTG plots recorded from powdered samples display three thermal processes which have been identi-fied [28] as follows: loss of water between 25 and about 250°C, decomposition of collagen and combustion of the residual organic components between 250 and 450°C and removal of carbonate ions from the inorganic phase be-tween 700 and 800°C (Fig. 1). While the peak tempera-tures exhibited by trabecular and cortical samples do not differ appreciably, the weight losses associated with the different peaks allow to determine an inorganic phase content of 62.0 ± 0.3% for trabecular bone and of 66.4 ± 0.3% for cortical bone, as reported in Table 1. Further-more, the carbonate content accounts for 2.3 ± 0.2% of the inorganic phase present in trabecular bone and 3.8 ± 0.2% in cortical bone (Table 1). The inorganic phases isolated from either trabecular or cortical bone samples exhibit X-ray powder diffraction patterns characteristic of poor crystalline hydroxylapatite (Fig. 2).

The step scanned x-ray diffraction patterns of the (310) and (002) reflections were used to evaluate the crystallite sizes. *D* values, which are related to the crystal size and strain in the long dimension (002) and the cross section (310) of the apatite crystals, were calculated from the width at half-maximum intensity ($\beta_{1/2}$) using the Scher-rer equation [29]

$$D = \frac{k\lambda}{\beta_{1/2} \cos \vartheta}$$

where λ is the x-ray wavelength and ϑ the diffraction angle. *K* is a constant varying with crystal habit and chosen as 0.9. The mean *D* values evaluated from the relative line broadening of the (002) and (310) reflections are reported in Table 2.

The infrared absorption spectra of deproteinated sam-ples show the absorption bands characteristic of poorly crystalline hydroxylapatite, together with the bands at 1455–1430 cm^{-1} and 870 cm^{-1} associated with the carbonate symmetric and out of plane stretching mode, respectively (Figs. 3a, c). The infrared absorption spectra of the samples heat treated up to 1000°C (Figs. 3b, d) show an overall increase of the sharpness of the absorp-
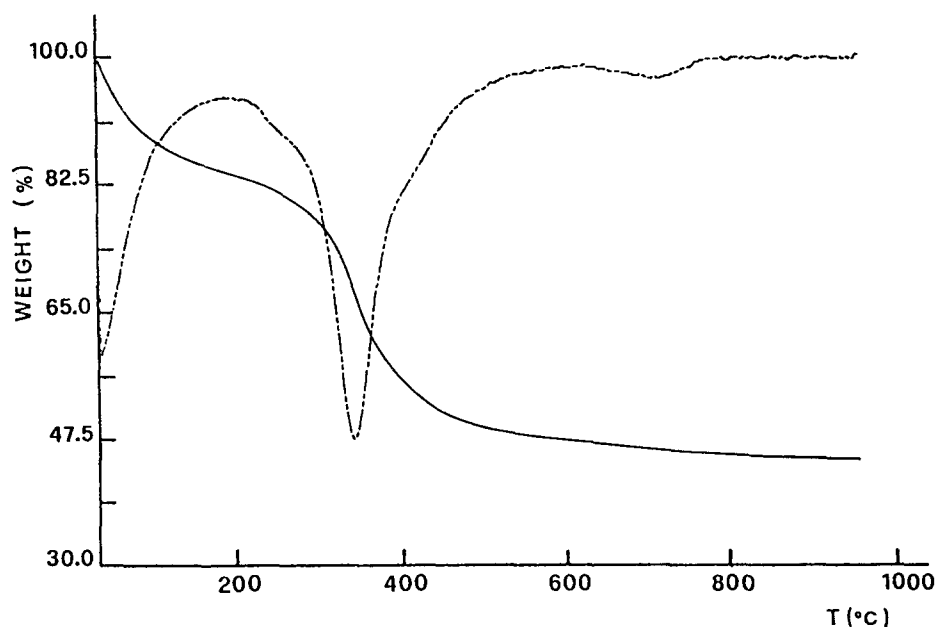
Figure 1. TG-DTG plot from a sample of trabecular bone.

tion bands. In particular, the absorption bands at 630 and 3572 cm^{-1} due to the libration and stretching mode of OH, respectively, become evident while the absorption bands characteristic of carbonate are no longer detectable. Furthermore, the presence of β-tricalcium phosphate (β-TCP) can be determined from the absorption bands at 1120, 970, and 940 cm^{-1}. In agreement, the powdered x-ray diffraction patterns of these samples indicate that heat treatment at 1000°C induces not only an overall increase in the degree of crystallinity of the apatitic phase, but also a partial conversion of the hydroxylapatite into β-TCP (Fig. 4). The percentage of the relative amount of β-TCP evaluated from the ratio of the areas of the most intense diffraction maxima of the two phases is 15% for trabecular and 10% for cortical deproteinated samples. The lattice constants of the apatitic phases evaluated from the patterns recorded from the samples heat treated at 1000°C and reported in Table 3 do not differ appreciably. The inorganic phases from trabecular and cortical bone exhibit striking different Ca/P molar ratios and very similar magnesium contents (Table 1).

Table 1. Inorganic Phase Contents of Trabecular and Cortical Bones. Carbonate and Magnesium Content, Together with Ca/P Molar Ratio of the Inorganic Phases Are Also Reported. Each Value Is the Mean of Ten Samples and Is Reported with Its Standard Deviation. P (Significance Level) Calculated for Pairs of the Mean Values Are Also Reported.

	Inorganic Phase Content (% wt)	CO$_3^{2-}$ Content (% wt)	Mg^{2+} Content (atom %)	Ca/P Molar Ratio
Trabecular	62.0 ± 0.3	2.3 ± 0.2	3.6 ± 0.2	1.50 ± 0.2
Cortical	66.4 ± 0.3	3.8 ± 0.2	3.7 ± 0.2	1.63 ± 0.2
	$P < 0.001$	$P < 0.001$	NS	$P < 0.001$

Discussion

The results of this investigation reveal several chemical and structural differences between the inorganic phases from cortical and trabecular bone. Among the most significant of those were the apatite mean crystal sizes, carbonate content, Ca/P molar ratio and thermal stability. Trabecular bone exhibited reduced apatite mean crystal sizes with respect to cortical bone, the reduction being more evident along the 002 than the 310 direction. In physiologically calcified tissues, apatite crystal sizes have been shown to increase with tissue maturation [9, 10, 30–32]; whereas they display higher values than age-matched controls in osteopetrotic metaphyses [33], and reduced values in the fragile bone characteristic of osteogenesis imperfecta [22]. The crystallinity of bone mineral has been found to increase rapidly with the age of an animal, while no great variation has been found for fractions of different density within a single age [32, 34]. Increasing average crystal size in normally growing bone has been suggested to be related to changes in ionic composition and mineral density [10, 17]. Our data confirm this hypothesis. In fact, we found that the relative amount of inorganic phase is slightly, but significantly, less in trabecular than in cortical bone. Furthermore, trabecular bone apatite contains a smaller amount of carbonate ions and exhibits a lower Ca/P molar ratio than cortical bone apatite. Types A and B carbonated apatites can be distinguished on the basis of their a-lattice parameters and i.r. spectra [11–13]. Unfortunately, the poor crystallinity of both trabecular and cortical bone apatites do not allow an accurate evaluation of their lattice constants. On the other hand, heat treatment to 1000°C causes not only an increase in crystallinity, but also the removal of carbonate ions from the apatitic phases which then exhibit very similar lattice constants. However, the positions of the relative absorption bands in the i.r. spectra from untreated samples indicate that, as
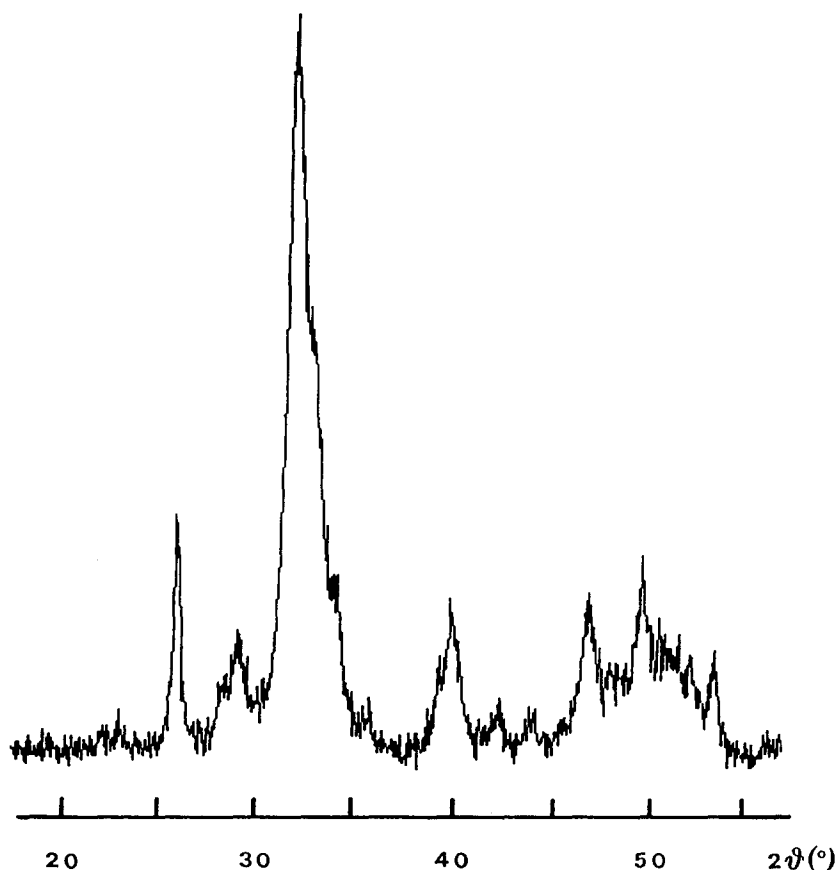
Figure 2. Powder x-ray diffraction pattern from a sample of deproteinated cortical bone.

in most biological apatites, some carbonate is substituted for phosphate, giving rise to the so called B carbonated apatites. The substitution of carbonate ions for phosphate groups in biological apatites has been associated with an increased stability of the apatite itself [35]. Furthermore, the presence of carbonate ions in synthetic apatites delays or prevents their thermal decomposition into β-TCP [15, 36]. In addition to magnesium, which favors the thermal conversion of apatite into β-TCP [5, 8, 9], another parameter affecting the thermal behavior of apatite is its Ca/P molar ratio [37]. In fact, stoichiometric apatites do not convert into any other phase on heat treatment up to 1000°C, while nonstoichiometric apatites do convert into β-TCP to an extent which increases as the Ca/P molar ratio decreases.

Table 2. Crystal Sizes (D_{hkl}) of Trabecular and Cortical Bone Apatites Evaluated from the Width at Half Maximum Intensity ($\beta_{1/2}$) of the (002) and (310) Reflections. Each Value Is the Mean of Ten Samples and Is Reported with Its Standard Deviation. P (Significance Level) Calculated for Pairs of the Mean Values Are Also Reported.

	$\beta_{1/2}(002)$ (°)	D_{002} (nm)	$\beta_{1/2}(310)$ (°)	D_{310} (nm)
Trabecular	0.481 ± 0.006	16.9 ± 0.2	1.26 ± 0.02	6.7 ± 0.1
Cortical	0.394 ± 0.006	20.7 ± 0.3	1.16 ± 0.02	7.3 ± 0.1
		$P < 0.001$		$P < 0.001$

Our data reveal that trabecular bone apatite exhibits a greater extent of thermal conversion into β-TCP than does cortical bone apatite. Since the magnesium level is almost the same in the two mineral phases, their different thermal behavior must be ascribed to the reduced carbonate content and, even more, to the reduced Ca/P molar ratio of trabecular bone apatite. In fact, while the Ca/P molar ratio in cortical bone is close to that of stoichiometric apatites, it is appreciably reduced in trabecular bone. It should be noted that the very low Ca/P molar ratio of trabecular bone apatite should cause an amount of thermal conversion greater than 15%. Since this does not occur, it can be concluded that the presence of > 2% by weight of carbonate in B sites must play a key role on the thermal stability of apatite, reducing the destabilizing effect of a nonstoichiometric Ca/P molar ratio.

On comparing our data with the characteristic changes of the inorganic phase during maturation of physiologically calcified tissues [10, 34] it can be inferred that trabecular bone has a lower degree of maturation with respect to cortical bone. It can be concluded that cortical and trabecular bone differ not only in the extent of collagen posttranslational modifications, which suggest a reduced stability of collagen fibrils from trabecular bone [24], but also in the structure and chemistry of their mineral phases. Therefore, functional differences in cortical and trabecular bone can be attributed to differences both in the matrix and in the mineral component.
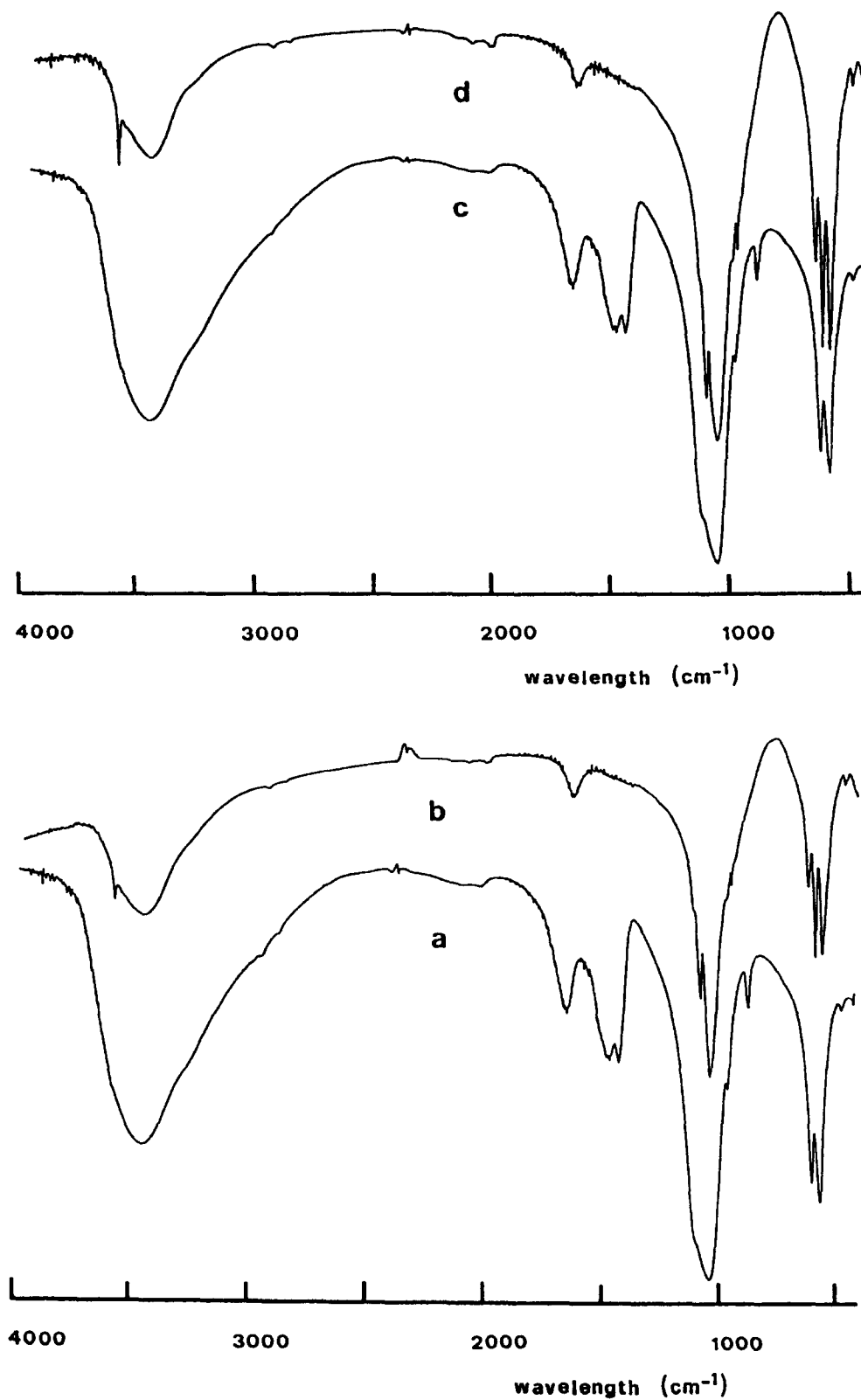
Figure 3. Infrared absorption spectra of deproteinated trabecular bone before (a) and after heat treatment at 1000°C (b), and of deproteinated cortical bone before (c) and after heat treatment at 1000°C (d).
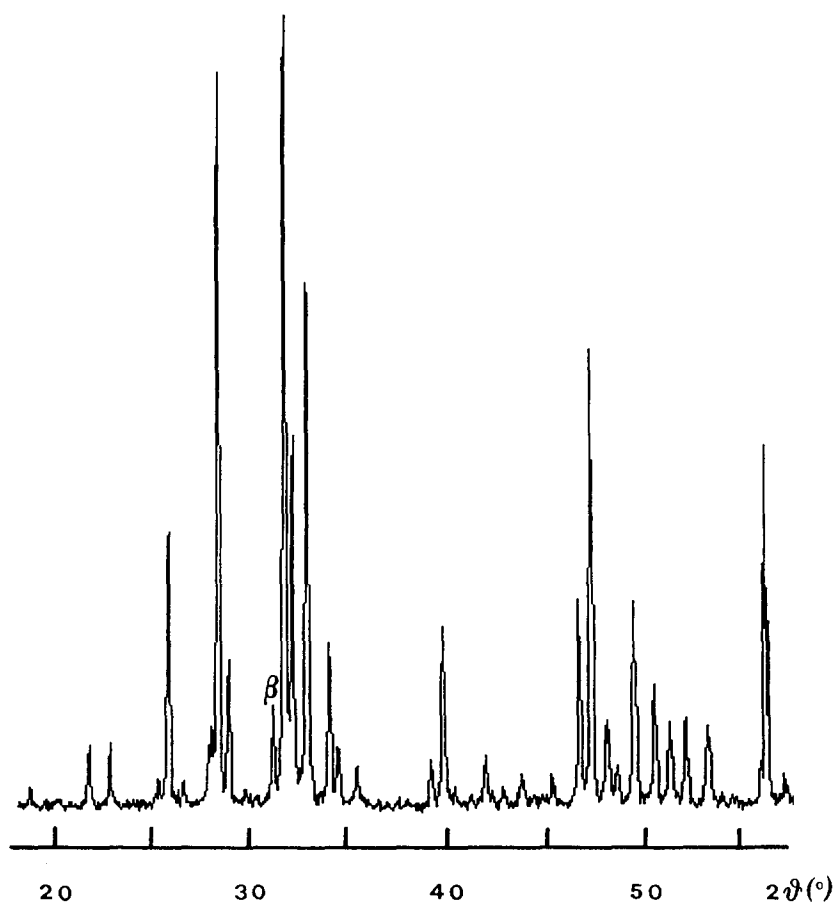
Figure 4. Powder x-ray diffraction pattern from a sample of deproteinated cortical bone heat treated at 1000°C. The most intense diffraction peak of β-tricalcium phosphate is indicated.

Table 3. Lattice Constants of the Hexagonal Apatitic Phases Evaluated from the Powder X-Ray Patterns of the Inorganic Phases Obtained by Heat Treatment at 1000°C of Trabecular and Cortical Bone Samples. Standard Deviations in Units of the Last Significative Figure Are Given in Parentheses.

	a-axis (Å)	*c*-axis (Å)	*V* (Å³)
Trabecular	9.415(2)	6.884(2)	528.4(2)
Cortical	9.418(4)	6.891(4)	529.3(4)

References

1. A. S. Posner, *Physiol. Rev.* **49**, 760 (1969).
2. C. A. Baud and J. M.Very, in *Role Calcium Biol. Syst. 1*, L. J. Anghileri and A. Tuffet-Anghileri, Eds., CRC, Boca Raton, FL, 1982, pp. 95–105.
3. M. C. Pugliarello, F. Vittur, B. de Bernard, E. Bonucci, and A. Ascenzi, *Calcif. Tissue Res.* **12**, 209 (1973).
4. R. Z. LeGeros and J. P. LeGeros, in *Phosphate Minerals*, J. O. Nriagu and P. B. Moore, Eds., Springer, New York, 1984, pp. 351–385.
5. A. Bigi, G. Falini, E. Foresti, M. Gazzano, A. Ripamonti, and N. Roveri, *J. Inorg. Biochem.* **49**, 69 (1993).
6. A. Bigi, G. Falini, E. Foresti, M. Gazzano, A. Ripamonti, and N. Roveri, *Acta Cryst.* **B52**, 87 (1996).
7. A. S. Posner, N. C. Blumental, and F. Betts, in *Phosphate Minerals*, J. O. Nriagu and P. B. Moore, Eds., Springer, New York, 1984, pp. 330–350.
8. A. Bigi, L. Compostella, A. M. Fichera, E. Foresti, M. Gazzano, A. Ripamonti, and N. Roveri, *J. Inorg. Biochem.* **34**, 75 (1988).
9. A. Bigi, E. Foresti, R. Gregorini, A. Ripamonti, N. Roveri, and J. S. Shah, *Calcif. Tissue Int.* **50**, 439 (1992).
10. J. M. Burnell, E. J. Teubner, and A. G. Miller, *Calcif. Tissue Int.* **31**, 13 (1980).
11. R. Z. LeGeros, O. R. Trauz, and J. P. LeGeros, *Science* **155**, 1409 (1967).
12. G. Bonel, *Ann. Chim.* **7**, 65 (1972).
13. J. C. Elliott, *J. Appl. Cryst.* **13**, 618 (1980).
14. S. Baravelli, A. Bigi, A Ripamonti, N. Roveri, and E. Foresti, *J. Inorg. Biochem.* **20**, 1 (1984).
15. F. Apfelbaum, I. Mayer, and J. D. B. Featherstone, *J. Inorg. Biochem.* **38**, 1 (1990).
16. C. Rey, M. Shimizu, B. Collins, and M. J. Glimcher, *Calcif. Tissue Int.* **46**, 384 (1990).
17. A. L. Arsenault and M. D. Grynpas, *Calcif. Tissue Int.* **43**, 219 (1988).
18. J. E. Roberts, L. C. Bonar, R. G. Griffin, and M. J. Glimcher, *Calcif. Tissue Int.* **50**, 42 (1992).
19. M. D. Grynpas, L. C. Bonar, and M. J. Glimcher, *Calcif. Tissue Int.* **36**, 291 (1984).
20. L. Cohen-Solal, L. Zylberberg, A. Sangalli, M. Gomez Lira, and M. Mottes, *J. Biol. Chem.* **269**, 14751 (1994).
21. J. P. Cassella and S. Yousuf Ali, *Bone and Mineral* **17**, 123 (1992).
22. U. Vetter, E. D. Eanes, J. B. Kopp, J. D. Termine, and P. Gehron Robey, *Calcif. Tissue Int.* **49**, 248 (1991).

23. E. F. N. Holland, J. W. W. Studd, J. P. Mansell, A. T. Leather, and A. Bailey, *Obstet Gynecol.* **83**, 180 (1994).
24. K. Noris Suarez, M. Romanello, P. Bettica, and L. Moro, *Calcif. Tissue Int.* **58**, 65 (1996).
25. M. J. Glimcher, in *Handbook of Physiology: Endocrinology* 7, R. O. Greep and E. B. Astwood, Eds., American Physiological Society, Washington, DC, 1976, pp. 25–113.
26. J. D. Termine, E. D. Eanes, D. J. Greenfield, M. U. Nylen, and R. A. Harper, *Calcif. Tissue Res.* **12**, 73 (1973).
27. K. P. Quinlan and M. A. De Sesa, *Anal. Chem.* **27**, 1626 (1955).
28. A. Bigi, A. Ripamonti, G. Cojazzi, G. Pizzuto, N. Roveri, and M. H. J. Koch, *Int. J. Biol. Macromol.* **143**, 110 (1991).
29. L. E. Alexander, in *X-ray Diffraction Methods in Polymer Science*, Wiley Interscience, New York, 1969.
30. R. G. Handschin and W. B. Stern, *Calcif. Tissue Int.* **51**, 111 (1992).
31. V. Ziv and S. Weiner, *Connect. Tissue Res.* **29**, 1 (1993).
32. L. C. Bonar, A. H. Roufusse, W. K. Sabine, M. D. Grynpas, and M. J. Glimcher, *Calcif. Tissue Int.* **35**, 202 (1983).
33. A. L. Boskey and S. C. Marks, *Calcif. Tissue Int.* **37**, 287 (1985).
34. C. Rey, V. Renugopalakrishnan, B. Collins, and M. J. Glimcher, *Calcif. Tissue Int.* **49**, 251 (1991).
35. G. H. Nancollas, in *Biological Mineralization and Demineralization*, Dahlem Konferenzen, Springer-Verlag, Berlin, 1982.
36. A. Bigi, E. Foresti, A. Ripamonti, and N. Roveri, *J. Inorg. Biochem.* **15**, 317 (1986).
37. A. Bigi, E. Foresti, M. Gandolfi, M. Gazzano, and N. Roveri, *J. Inorg. Biochem.* **58**, 49 (1995).